A SYSTEM STUDY ON SILICON THIN-FILM pm-Si:H/µc-Si:H TANDEM CELL STRUCTURE

F. Dadouche (1), O. Béthoux (1), E. Labouré (1), E. Johnson (2), P. Roca i Cabarrocas (2), C. Marchand (1), J.-P. Kleider (1)

(1) Laboratoire de Génie Electrique de Paris, CNRS UMR8507; SUPELEC; Univ Paris-Sud; UPMC Univ Paris 6; 11 rue Joliot Curie, Plateau de Moulon, F-91192 Gif-sur-Yvette Cedex, France
(2) Laboratoire de Physique des Interfaces et Couches Minces, CNRS, Ecole Polytechnique, 91128 Palaiseau Cedex, France

ABSTRACT:

This article aims to optimize an innovative tandem structure based on polymorphous and microcrystalline silicon for the top and bottom elementary cells, respectively, combined with an original DC-DC converter. The studied tandem structure is composed of two separated cells. Each of them is connected to its own electrodes. Thus they are electrically decoupled but optically coupled. In those conditions, the constraint of current matching usually needed in the classical micromorph structures is released. As a result, the robustness against the current variations is enhanced and the efficiency of the structure improves.
Since the top cell plays the main role in the determination of the transmitted part of the incoming flux to the bottom cell, the thickness of the intrinsic layer of the polymorphous cell is tuned so that the output power of the global structure becomes maximal.
To implement the electric decoupling of two sub cells, the studied structure needs two static converters. In order to minimize the converters bulk, an innovative output electric architecture and its optimized related control is designed. This systemic approach leads to a better global structure in terms of efficiency, cost and management.

Keywords: silicon, pm-Si:H, µc-Si:H, 4-wire tandem structure, DC-DC-Converter.

1 INTRODUCTION

In order to fulfil the goals that society requests (environmental stresses cut-off), photovoltaic industry must become a major electricity supplier in the twenty-first century. To achieve this goal, photovoltaic generators must overcome three main challenges: a dramatic fall of cost ($/$W_P$), also an increase in cell and module efficiency (Wp/m^2) and lastly a more flexible management of the overall energy output. One needs especially to insure that each cell operates, at any time, at its optimal power point whatever the electrical load or the environmental conditions.

Our work focuses on this latter issue and proposes new ways of integrating the power electronics devices close to the modules. For that purpose, we consider thin film silicon multijunction solar cells and more precisely the tandem association of hydrogenated polymorphous (pm-Si:H) and microcrystalline silicon (µc-Si:H) component cells. Three arguments bear out this choice: silicon is a widespread raw material, thin-film technology is a low-energy consumption process and tandem cells are more efficient than single cells because they are able to convert a wider range of solar photons.

In a previous work, it has been discussed the best choice for cell association in tandem structures [1]. Two ways of associating the cells were studied and compared: (i) the classical structure in which the two cells are electrically and optically coupled, called the 2-wire structure, and (ii) an innovative structure for which the electrical constraint is relaxed by the electrical decoupling of the two cells, called the 4-wire structure (Figure 1). Our study led to the conclusion that the 4-wire structure is, in any case, better than the traditional association. Moreover, we can argue on a much more robust maximum power point.

Since the 4-wire structure needs two static converters (one for each sub cell) it is mandatory that their dimensions be as small as possible. Hence it is interesting to respond to this constraint by showing how to design these converters and integrate them close to the module. As a matter of fact, the bulkier part of such converters is their passive components (inductors and capacitors). That is the reason why we take profit of all the degrees of freedom. We first propose to interleave the converters control signals. This leads to a reduction of the output capacitors but not of the input inductors. Secondly, in order to also decrease this component size, we suggest an original electro-magnetic coupling of the two coils.

We here present a system study combining the 4-wire tandem structure with an original static converter. After introducing the studied structure as well as the associated static converter, we present the simulation procedure adopted to optimize the structure so that the output power will be maximal. Then we extract results which will be discussed in the last section.

2 STUDIED STRUCTURE

The tandem cell concept consists in putting together in the same structure two solar cells made of materials that have different bandgap energies, in order to better match the bandgap to the energy of the incoming photons. The bottom cell is made of materials with a low bandgap such as microcrystalline silicon and the top cell materials have higher band gap such as amorphous and polymorphous silicon. This structure permits to extend the spectral range of high collection efficiency [1, 2]. Indeed the top cell has a good photo response in the blue region while the bottom cell is more efficient in the red

and infrared regions.

In this work the top cell is made of polymorphous silicon because of its proven better electronic properties and better stability compared to the conventional amorphous silicon [3-6]. In addition the optical bandgap of pm-Si:H is slightly larger than the a-Si:H one. Moreover, due to its higher absorption coefficient in the visible range, a pm-Si:H thickness of only a few hundreds of nanometres is required, while the lower absorption coefficient of µc-Si:H imposes a thicker intrinsic layer.

The 4-wire structure studied here consists of two independent cells (pm-Si:H and µc-Si:H) which are electrically decoupled while being optically coupled. Indeed each of the two sub cells needs its own two electrodes connected to each P and N layers (Fig. 1b). The advantage of this structure compared to the classical one, made by successive layer deposition (Fig. 1a), is that the two sub cells can work with different currents and so there is no need to match their currents. This leads to a more efficient structure [1].

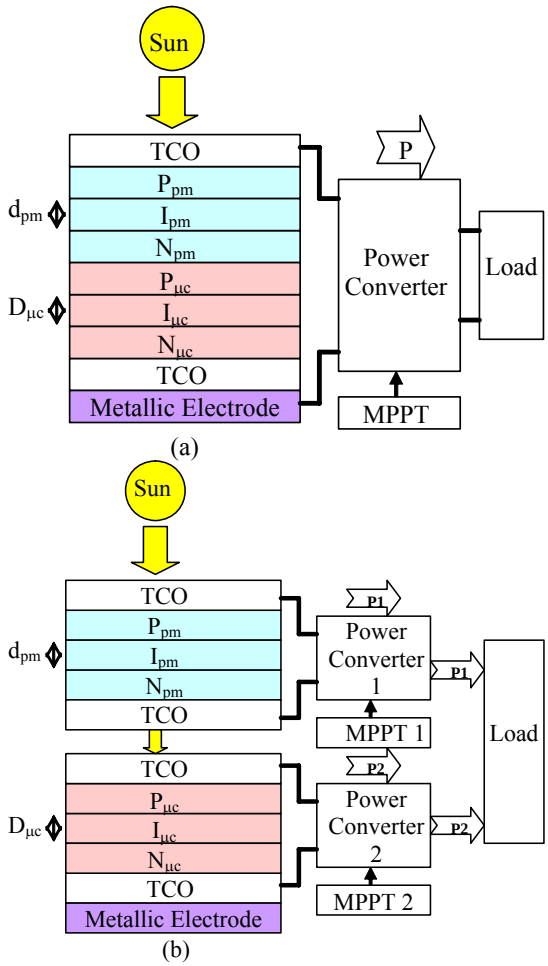

Figure 1: The two kinds of tandem association and the associated power converter: (a) 2- wire structure; (b) 4-wire structure.

As the two cells of this structure are electrically decoupled, this design needs a dedicated architecture to add the electric powers provided by the top and the bottom cells. Thus, each sub-cell supplies its power to the external load through an associated power converter. This enables that both blocks, made of sub-cell and sub-converter, can have either the same current (which leads to series connection) or the same voltage (which leads to parallel connection).

As depicted in Fig. 2, the converter can be either a voltage step-up (boost converter) or a voltage step-down (buck converter) device. As photovoltaic cells are low voltage power sources and loads are high voltage devices, in order to reduce Joule effect losses, it is mandatory to use a boost converter at the output of a photovoltaic module. In this case the output voltage V_O is related to the photovoltaic voltage V_{PV} as follows:

$$V_O = \frac{V_{PV}}{1-d}$$

with d the controlled switch PWM duty cycle.

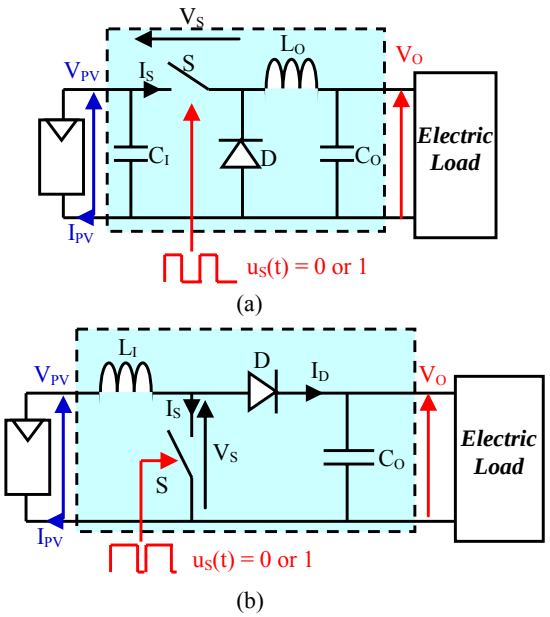

Figure 2: The two types of power converter: (a) the buck converter, and (b) the boost converter.

The two independent boost converters can be associated either in parallel or in series (Fig. 3). Each connection is suitable for independent power tracking. Indeed the load uses the sum of bottom and top powers by utilizing a global voltage regulation.

In the parallel case, each MPPT algorithm computes its PWM duty cycle d_k that enables its cell to work at its maximum power point:

$$d_k = 1 - \frac{(V_{PVk})_{MPP}}{V_O}$$

It ensures no delay compared to a single cell maximum power tracking. As the maximum power voltage range is not so large, the duty cycle range is not considerable, which is a good point for power converter design optimization.

In the series case, each MPPT algorithm computes its PWM duty cycle d_k the same way, but, in this circumstance, d_k evolves in a large scale. Its value is determined as follows:

$$d_k = 1 - \frac{(V_{PVk})_{MPP}}{(V_O)_k}$$

with $(V_O)_k$ determined by a power balance. The intermediate capacitor current $(i_{CO})_k$ is definitely the difference of the converter number k output current and the load current i_{load}. Consequently, $(V_O)_k$ can be calculated as:

$$(V_O)_k = \frac{(P_{PVk})_{MPP}}{i_{load}}$$

Hence, in case of cells mismatching (ageing effects, environmental conditions as temperature or light spectrum…), $(V_O)_k$ can vary a lot inducing a duty cycle wide range which is negative as far as power device design is concerned (with respect to control and power efficiency). Consequently, this study is based on the parallel connection of boost converters.

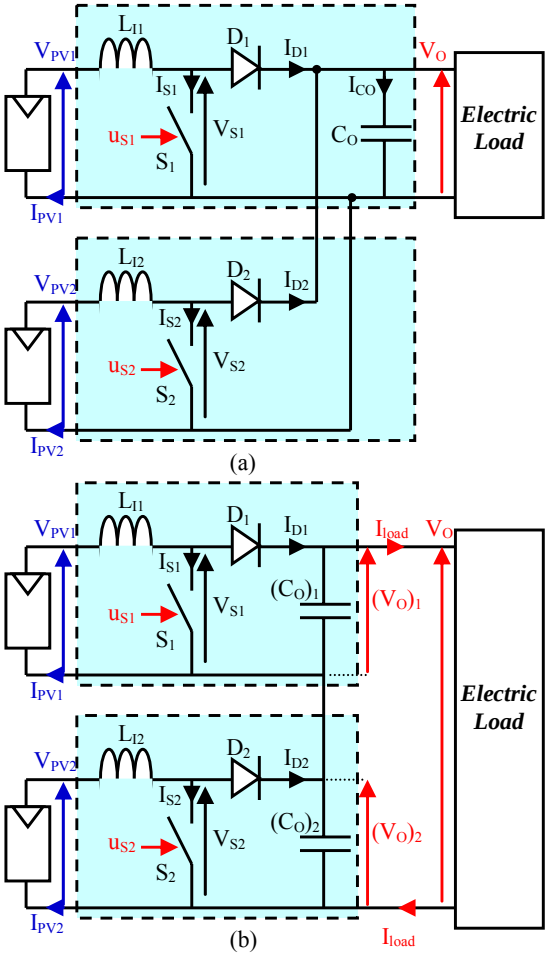

Figure 3: The two types of power converter connections: (a) boost converters in parallel, and (b) boost converters in series.

3 SIMULATION TOOLS AND PROCEDURE

The simulation of the studied structure is performed in two successive steps using two different tools. First the pm-Si:H/µc-Si:H structure without its associated converter is optimized so that it produces the maximum power. Then, after computing the corresponding output current and voltage for both top and bottom cells, we design the associated optimized converter.

To optimize the studied structure and evaluate its output power we mainly used a numerical simulation software developed by the Hahn-Meitner Institut (now Helmholtz Zentrum) in Berlin. The software called "AFORS-HET" (Automat FOR Simulation of HETero-structures) is primarily dedicated to heterojunction solar cells [7]. However, it allows one to extract different macroscopic characteristics in dark conditions or under sun illumination for any type of solar cells. It enables to introduce different profiles of defects in the energy band gap of each layer constituting the cell.

To optimize the studied electric architecture (boost converters connected in parallel), the widespread matlab/simulink interface is used. It allows one to implement both any control law (Maximum Power Point Tracking in our case) and any converter (currently boost converter) by taking advantage of the power dedicated toolbox called "Sim Power Systems library". It also facilitates curves drawing and waveform analyses (Fast Fourier Transform …) [8].

3.1 Optimization of the pm-Si:H/µc-Si:H structure

The first step consists in tuning the thicknesses of the different layers of the top and bottom cells in order to obtain the maximum output power of the structure. The incident flux first goes through the top pm-Si:H cell, which absorbs part of the photons and transmits the remaining part to the bottom cell. Consequently, the top cell plays the main role and the thickness of its I active layer must be determined accurately. The role of the P- and N- layers is to create the junctions and the internal electrical field through the intrinsic layers with a minimum of absorption, so they must be chosen as thin as possible. For the thickness of the microcrystalline intrinsic layer, it can be fixed to reasonable value, sufficiently large to absorb most of the output flux coming from the top cell. For silicon thin film tandem structures, this layer width is generally larger than one micron, so it is fixed at 1.5 µm. The thicknesses of all the layers are given in Table I.

Table I: Thicknesses of the different layers of pm-Si:H and µc-Si:H cells introduced in simulation

	pm-Si:H cell		µc-Si:H cell	
	Material	Thickness (nm)	Material	Thickness (nm)
P-Layer	a-SiC:H	15	µc-Si:H	25
I-layer	pm-Si:H	variable	µc-Si:H	1500
N-layer	a-Si:H	20	a-Si:H	20

The key factor determining the thickness of the intrinsic layer of the pm-Si:H cell is the ageing process happening during the first months of illumination, called light-soaking. It is known that amorphous silicon thin films are characterized by two kinds of defects: the network defects linked to the weak bonds and the deep defects linked to the dangling bonds. According to the Staebler-Wronsky effect, under illumination, some weak bonds are broken leading to the creation of new dangling bonds [9].

The first kind of defects is usually modelled by two exponential bandtails situated in both sides of the bandgap. The second one, even if it is known to be of amphoteric type [10], can be modelled by two Gaussian

continuous distributions of monovalent states [11, 12].

In order to account for the light-soaking phenomenon on the performance of the pm-Si:H cell, we modelled the creation of new dangling bonds by increasing the magnitude of the Gaussian distributions (D_{max}) without varying their widths. Figure 4 illustrates the variations of pm-Si:H cell efficiency against the pm-Si:H intrinsic layer thickness for different values of D_{max} introduced in the simulation.

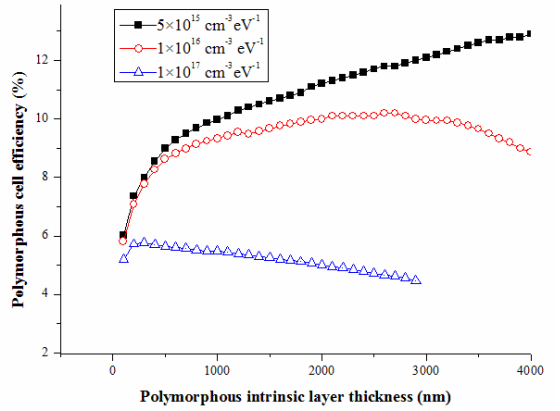

Figure 4: pm-Si:H cell efficiency as a function of pm-Si:H intrinsic layer thickness for three values of the peak value, D_{max}, of the Gaussian distributions of deep defects: 5×10^{15} $cm^{-3}eV^{-1}$, 1×10^{16} $cm^{-3}eV^{-1}$, 1×10^{17} $cm^{-3}eV^{-1}$.

One can observe the decrease of the cell efficiency by increasing D_{max} for a given thickness. This is due to the decrease of carrier diffusion length and screening of the electric field when the density of deep defects is increased. In addition, for a given D_{max} the cell efficiency first increases with the increase of the intrinsic layer thickness up to an optimal value, and then decreases (the decrease occurs at larger thickness for the lowest defect density and is not visible on this figure). This is due to two phenomena acting concurrently: (i) on the one hand the widening of the intrinsic layer leads to the increase of photogenerated carriers (ii) on the other hand the chance for the created carriers to recombine before reaching the electrodes gets larger. Since the latter also gets larger when the defect density is increased, the optimal thickness decreases when the defect density increases.

From this simulation the location of the optimal thickness is determined for different states of the pm-Si:H materials as reported in table II.

Table II: Optimal thicknesses of the intrinsic pm-Si:H layer in different states.

State	D_{max} (cm^{-3} eV^{-1})	Optimal thickness (µm)
As deposited	5×10^{15}	beyond 4
Intermediate	1×10^{16}	2.7
Light-soaked	1×10^{17}	0.3

To take into account the degradation caused by light soaking it is necessary to limit the thickness of the intrinsic layer of the pm-Si:H cell to values lower than 500 nm. With regards to this conclusion, to estimate the output power of the studied tandem structure, we optimized the intrinsic layer thickness of the top cell in the interval [50 nm, 450 nm].

The procedure adopted to perform our simulation is illustrated by Fig. 5 and summarized as follows:

1. Application of standard AM1.5 illumination as an input flux of the top pm-Si:H cell.
2. Variation of the intrinsic layer thickness of the top cell from 50 nm to 450 nm with a step of 50 nm.
3. Calculation of the output flux of the pm-Si:H cell for each thickness.
4. This last one is introduced as an input flux of the µc-Si:H cell.
5. Computation of J-V and P-V curves for both cells.
6. Finally using the P-V curves, the maximum power is determined by adding the maximum power of elementary cells.

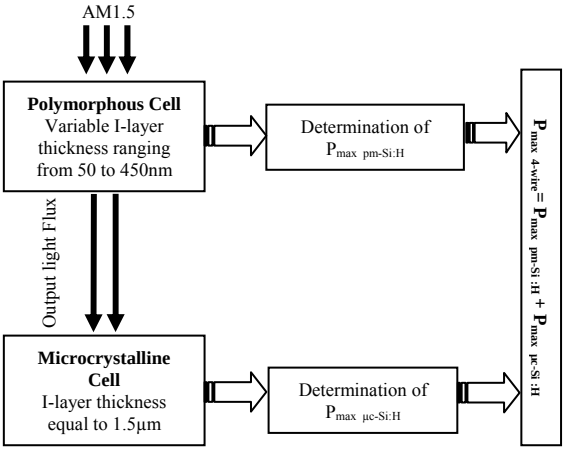

Figure 5: Simulation steps for the 4-wire tandem structure.

3.2 Static converter design and optimization

The two objectives of the control scheme are to track the maximum power point of both cells (P_{MPP1} and P_{MPP2}) whatever the load requirements and the environmental conditions. For that purpose, the control algorithm can settle the PWM commands $u_{S1}(t)$ and $u_{S2}(t)$. These two variables provide three degrees of freedom. As a matter of fact, while operating at the same switching frequency F_S, they are characterized by their own duty cycles d_1 and d_2 as well as the phase shift $\varphi_{1/2}$ between $u_{S1}(t)$ and $u_{S2}(t)$. As explained in section 2, the duty cycles d_1 and d_2 are computed in order to fulfil the maximum power requirements.

$$d_k = 1 - \frac{(V_{PVk})_{MPP}}{V_O}$$

The remaining degree of freedom $\varphi_{1/2}$ can be used for further optimization. As the studied converters have to be integrated as close as possible to the photovoltaic module, their dimensions are a design key point. For this reason, it is important to minimize passive components size (inductors and capacitors). Plotting both PWM command $u_{Sk}(t)$ and boost output current $i_{Dk}(t)$, one can

denote that this last waveform is a square shape with F_S frequency, (1-d_k) duty cycle and I_{PVk} magnitude (Fig. 6). As any cyclic variable, $i_{Dk}(t)$ can be written as a Fourier series. The computation leads to the following expression:

$$i_{Dk}(t) = (1-d_k)I_k + 2(1-d_k)I_k \sum_{\ell=1}^{\infty} \frac{\sin(\ell d_k \pi)}{\ell d_k \pi} \cos(\ell \omega_S (t - T_k))$$

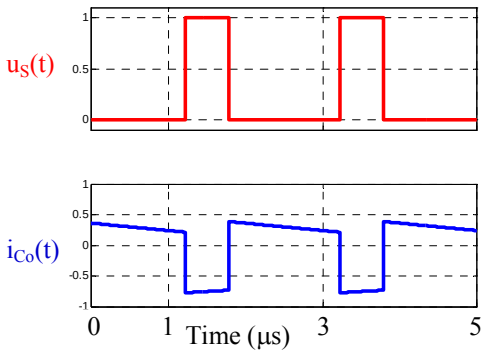

Figure 6: PWM control value and output capacitor current.

Since the output capacitor function is to filter any switching frequencies, one can assume that its current is:

$$i_{CO}(t) = 2(1-d_1)I_1 \sum_{\ell=1}^{\infty} \frac{\sin(\ell d_1 \pi)}{\ell d_1 \pi} \cos(\ell \omega_S (t - T_1))$$
$$+ 2(1-d_2)I_2 \sum_{\ell=1}^{\infty} \frac{\sin(\ell d_2 \pi)}{\ell d_2 \pi} \cos(\ell \omega_S (t - T_2))$$

Hence, the optimal choice is:

$$\begin{cases} (1-d_1)I_1 = (1-d_2)I_2 \\ T_2 - T_1 = \dfrac{T_S}{2} \end{cases}$$

The first equation is consistent with our main goal. The second one settles the last degree of freedom, the phase shift value ($\varphi_{1/2}$) in this case.

4 RESULTS AND DISCUSSION

The simulation results are divided in two sets: (i) the first concerns the studied structure including individual cells results after light soaking (ii) and the second is dedicated to the associated converter.

4.1 Elementary cells and 4-wire structure results

For the first set, the maximum output power of the two sub cells as well as that of the global structure against the pm-Si:H intrinsic layer thickness are presented in Fig. 7. Then the electrical characteristics (J-V) curves of the top and bottom cells for two values of the top intrinsic layer thickness are reported on Fig. 8.

From Fig. 7 one can extract the suitable thickness of the pm-S:H intrinsic layer to obtain the maximum output power of the structure. This depends on the performance of both top and bottom cells. For the top cell, as we have introduced it previously, as a result of the ageing process during light soaking, the light-soaked stabilized pm-Si:H cell presents an optimal value which is located in our case around 300 nm. On the contrary, since the microcrystalline cell is not affected by this process, its performance depends only on the fraction of flux transmitted by the top cell. Consequently, the thinner the top cell, the better the bottom cell efficiency. The combination of the two results explains that the optimal thickness for the pm-Si:H (I) layer in the tandem association is lower than for the pm-Si:H cell alone, and it is found around 200 nm.

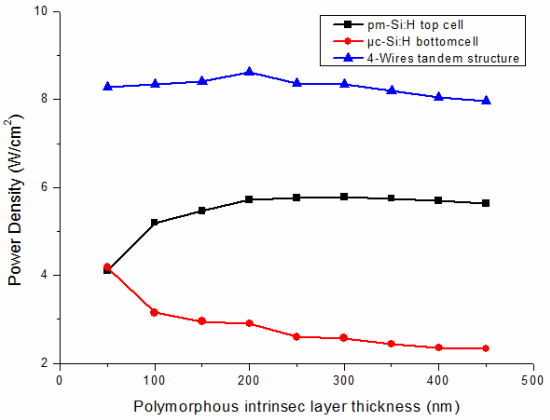

Figure 7: Maximum outputs of elementary cells as well as the global tandem structure versus polymorphous intrinsic layer thickness.

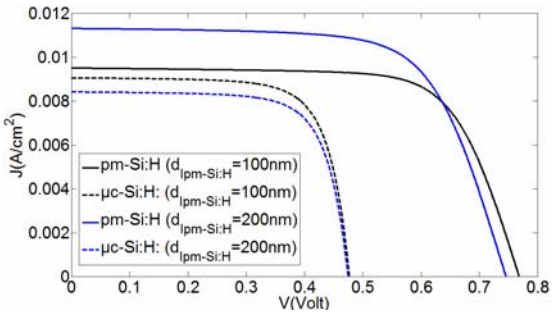

Figure 8: J-V curves of both pm-Si:H and µc-Si:H cells for two different pm-Si:H I-layer thicknesses.

Looking at the J-V curves sketched in Fig. 8, one can observe that for the optimal thickness determined before (200 nm), the current in the two cells is not matched. This means that to obtain the maximum power provided by the global structure it is necessary to exploit each cell independently. In addition to a better electric power, the 4-wire structure is much more robust against current variations because it is no more constrained by the matching condition, as opposed to the classical 2-wire tandem structure, which is thus more sensitive to current fluctuations caused by any outdoor conditions or manufacturing process.

4.2 Associated static converter results

In this section the simulation results of the electrical architecture are presented. This study is based on the previous values extracted from 4-wire structure simulations. As introduced before, the main parameters

are the voltage and current of both cells corresponding to the maximum output power of the global structure. These values are summarized in the table III. The following simulations are based on a top module made of twenty elementary top cells of roughly 1 A. The bottom module also consists of twenty elementary bottom cells of roughly 0.75 A. These values are calculated according to table III and considering that both top and bottom cells have the same area.

Table III: Maximum Power peak for elementary cells.

	$V_{MP\ peak}$ (mV)	$I_{MP\ peak}$ (mA)
pm-Si:H cell	567.5	10.08
µc-Si:H cell	386.2	7.52

The switching frequency F_S is fixed at 500 kHz, the inductors values are set to $L_{I1} = L_{I2} = 50$ µH and the output capacitor value is $C_O = 500$ nF. The variations of output capacitor current and voltage are reported on Fig. 9.

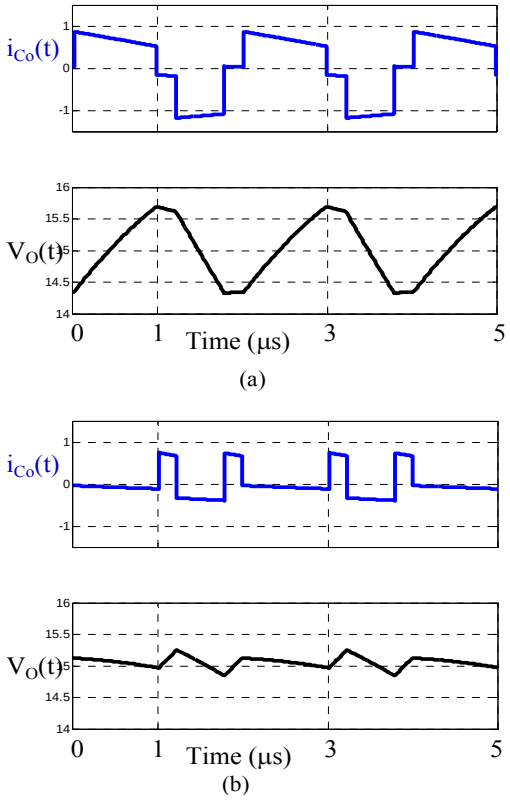

Figure 9: Output capacitor current and voltage: (a) phase shift equal to 0, and (b) phase shift equal to π.

Figure 9-a illustrates an inappropriate tuning corresponding to a phase shift value of 0 and leading to a large current magnitude at the switching frequency F_S. On the contrary Fig. 9-b shows the optimal case; the phase shift value is equal to π. This set of control parameters leads to a much smaller current magnitude with a very small fundamental frequency F_S; the main harmonic component is obviously 2 F_S, a frequency which is hence twice easier to filter. That is the reason why the output voltage ripple is drastically reduced in this optimal case.

By choosing both parallel connection and interleaving technique of the control signals, it is possible to minimize the output filter (output capacitor) dimensions and improve efficiency. But the input part of the converter behaves as if there was a single converter. Therefore the interleaving technique does not lead to any current ripple decrease. In order to reduce the inductors bulk, these input inductors can be interlaced [13-17]. By building them on a same magnetic core, we introduce a transformer instead of two inductors (Fig. 10). This transformer is characterized by self inductances L_1 and L_2 and the mutual inductance M.

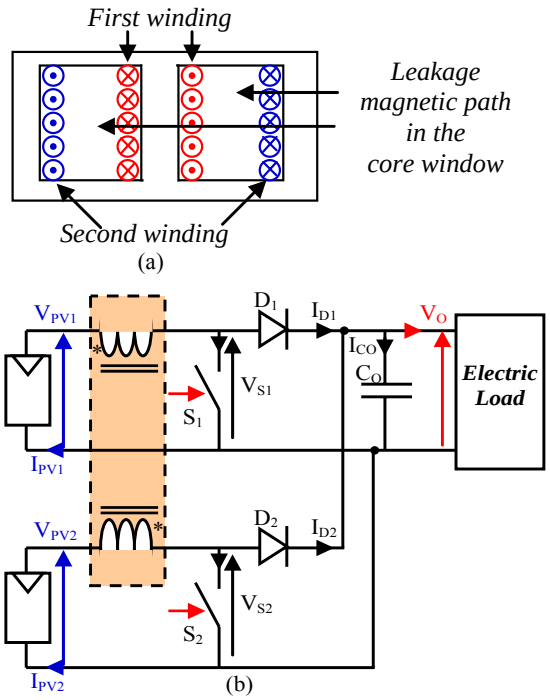

Figure 10: The proposed power converter :(a) the coupled inductors, and (b) the interleaved power converter.

In this case, DC component and low frequency current are filtered by the leakage inductance. This last one is designed by choosing the leakage magnetic path in the winding core window. Most of the high frequency current (linked to switching ripples) are filtered by the mutual inductance which value is much larger than the basic inductor value. As a result this latter must have a low permeability material in order to store the DC energy ($1/2 \times LI^2$). Consequently, this design choice leads to a small inductor value whereas the transformer doesn't face the same constraint.

The input current waveforms are reported on Fig. 11-a; the signals present high current ripples at the switching frequency F_S. By integrating the two inductors into a same transformer, this frequency almost disappears and the current ripples magnitude is hence much smaller (Fig. 11-b). The transformer has the same leakage inductance $L_{leakage} = 50$ µH, but its mutual inductance is much higher $M = 5$ mH.

5 CONCLUSION

In this work a simulation study of an innovative tandem pm-Si:H/µc-Si:H structure associated to an original converter is performed.

First the structure is optimized in order to extract the maximum output power of each individual cell. Taking account of the light-soaking process, the optimal thickness of the intrinsic pm-Si:H layer in the top cell was found to be around 200 nm. For this thickness the current is not matched between the two sub-cells. So in order to achieve the best performance with different cell currents, it is mandatory to associate for each cell its own converter. In addition this implementation permits that the global structure is far less sensitive to operating conditions (temperature, light spectrum…). Thus the 4-wire structure is not constrained by the current matching condition which is mandatory in the case of a classical 2-wire tandem structure. This confirms the good performance of this structure and its robustness against current variations which can be the result of outdoor conditions or manufacturing process.

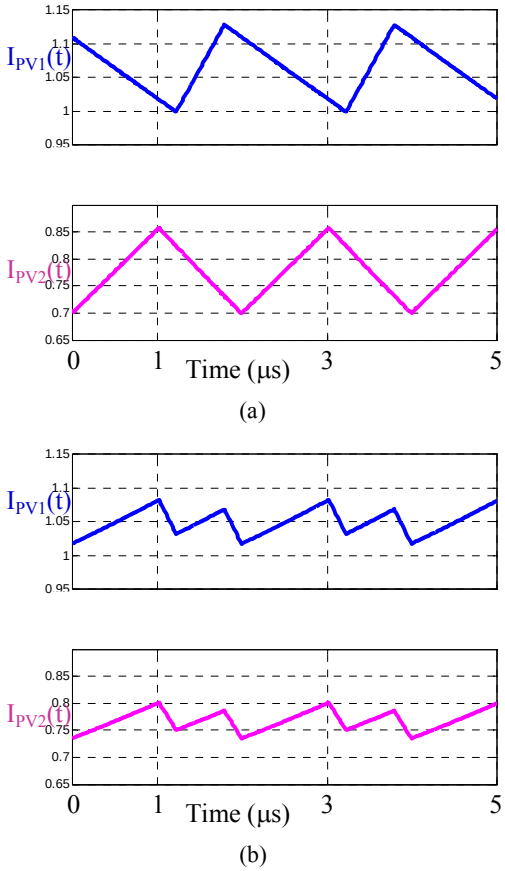

Figure 11: Photovoltaic array currents: (a) with classic coil inductors, and (b) with intercell transformer.

Second, this innovative tandem cell design is built in association with power converters. For this purpose, the different converters and their combinations are explored in order to design very compact electric output architecture. This leads to the choice of boost converters. In order to take advantage of the interleaving technique the converters outputs are associated in parallel. The innovative part of the study is that we have also associated the input inductors. This approach allows the converters to reduce their input filter bulk. Optimizing the boost control values by interleaving them, we hence succeed to dramatically reduce both output capacitor value and input core size.

ACKNOWLEDGEMENTS

This work was partly supported by ANR (Agence Nationale de la Recherche) in the framework of the ATOS project.

6 REFERENCES

[1] F. Dadouche, O. Béthoux, M.E. Gueunier-Farret, E.V. Johnson, P. Roca i Cabarrocas, C. Marchand and J.P. Kleider, E-MRS Spring meeting, 2009.
[2] P.D. Veneri, P. Aliberti, L.V. Mercaldo, I. Usatii, C. Privato, Thin Solid Films 516 (2008) 6979.
[3] C. Longeaud, J.P. Kleider, P. Roca i Cabarrocas, S. Hamma, R. Meaudre, M. Meaudre, J. Non-Cryst. Solids 227-230 (1998) 96.
[4] R. Butté, R. Meaudre, M. Meaudre, S. Vignoli, C. Longeaud, J.P. Kleider, P. Roca i Cabarrocas, Philos. Mag. B 79 (1999) 1079.
[5] M. Meaudre, R. Meaudre, R. Butté, S. Vignoli, C. Longeaud, J.P. Kleider, P. Roca i Cabarrocas, J. Appl. Phys. 86 (1999) 946.
[6] J.P. Kleider, C. Longeaud, M. Gauthier, M. Meaudre, R. Meaudre, R. Butté, S. Vignoli, P. Roca i Cabarrocas, Appl. Phys. Lett. 75 (1999) 3351.
[7] R. Stangl, A. Froitzheim, M. Kriegel, T. Brammer, S. Kirste, L. Elstner, H. Stiebig, M. Schmidt, W. Fuhs, Proceedings 19th European Photovoltaic Solar Energy Conference (2004) 1497.
[8] D. M. Smith, Engineering Computation with MATLAB, Addison-Wesley, 2009, 2nd edition.
[9] D.L. Staebler and C.R. Wronsky, Appl. Phys. Lett. 31 (1977) 292.
[10] R.A. Street, in Hydrogenated Amorphous Silicon; Cambridge University Press, 1991.
[11] R. Martins, A. Fantoni, M. Vieira, J. of Non-Cryst. Solids 164-166 (1993) 671.
[12] P. Chatterjee, J. Appl. Phys. 76 (1994) 1301.
[13] A. M. Schultz and C. R. Sullivan, US Patent No 6362986 (2002).
[14] J. Li, C. R. Sullivan and A. M. Schultz, Proc. IEEE APEC Conf. (2002) 817.
[15] P. Zumel, O. Garcia, J. A. Cobos and J. Uceda, Proc. IEEE APEC Conf. (2003) 1143.
[16] T. Meynard, F. Forest, E. Labouré, V. Costan, A. Cunière, E. Sarraute, Proc IEEE CIPS Conf. (2006).
[17] F. Forest, T. Meynard, E. Labouré, V. Costan, A. Cunière, T. Martiré, IEEE Transactions on Power Electronics 22 (2007) 934.